J Therm Anal Calorim (2012) 109:131–139
DOI 10.1007/s10973-011-1692-5

Thermoanalytical, magnetic and structural study of Co(II) complexes with substituted salicylaldehydes and neocuproine

Maria Lalia-Kantouri · Maria Gdaniec · Agnieszka Czapik · Konstantinos Chrissafis · Wieslawa Ferenc · Jan Sarzynski · Christos D. Papadopoulos

Received: 16 February 2011 / Accepted: 24 May 2011 / Published online: 16 June 2011

Abstract In this study, simultaneous TG/DTG-DTA technique was used for two cobalt(II) complexes with neocuproine(neoc) and the anion of a substituted salicylaldehyde ligand (X-salo) (X = 3-OCH_3, or 5-CH_3) with the general formula [Co(X-salo)$_2$(neoc)], to determine their thermal degradation in inert atmosphere, which was found to be a multi-step decomposition related to the release of the ligand molecules. The solid material at 1300 °C (verified with PXRD) was a mixture of carbonaceous metal cobalt. Evolved gas analysis by coupled TG-MS verified the elimination of a formaldehyde molecule in the first decomposition stage, initially proposed by the percentage mass loss data. By single-crystal X-ray diffraction analysis an octahedral geometry of the complex [Co(3-OCH_3-salo)$_2$(neoc)] was found. The variable temperature magnetic susceptibility measurements showed a paramagnetic nature of the complexes, in accordance with their molecular structure. Finally, for the determination of the activation energy (*E*) two different methods (the isoconversional methods of Ozawa, Flynn and Wall (OFW) and Friedman) were used comparatively.

Keywords Crystal structure · TG/DTG-DTA · Kinetics · Cobalt complexes · Salicylaldehydes · Neocuproine · Magnetics · TG-MS

Introduction

The strong coordinating properties of 2-hydroxy-benzaldehydes (salicylaldehyde, saloH) and their derivatives with 3d transition metals have stimulated research on these compounds, which find applications in both pure [1] and applied chemistry fields, such as in extractive metallurgy as analytical reagents [2] and specifically for cobalt compounds in tyre industry as adhesion promoters [3]. These ligands are known to coordinate in a bidentate manner with transition metals in the mono-anionic form, adopting square-planar [4–6] or octahedral geometry [7]. It is recently found, however, by us that under proper conditions, 3-OCH_3-salicylaldehyde with Fe(III) ion can coordinate with two different modes and as bridging ligand, forming polynuclear complexes [Fe_2(3-OCH_3-salo)$_8$-Na_5]8H_2O [8], while 2-OH-benzophenones give the simple complexes [Fe(2-OH-benzophenone)$_3$] [9]. On the other hand, it is well known that cobalt chelates with α-diimines

---

Electronic supplementary material The online version of this article (doi:10.1007/s10973-011-1692-5) contains supplementary material, which is available to authorized users.

M. Lalia-Kantouri (✉) · C. D. Papadopoulos
Department of Chemistry, Lab of Inorganic Chemistry, Aristotle University of Thessaloniki, P.O. Box 135, 54 124 Thessaloniki, Greece
e-mail: lalia@chem.auth.gr

M. Gdaniec · A. Czapik
Faculty of Chemistry, Adam Mickiewicz University, 60780 Poznan, Poland

K. Chrissafis
School of Physics, Solid State Physics Department, Faculty of Science, Aristotle University of Thessaloniki, 54 124 Thessaloniki, Greece

W. Ferenc
Department of General and Coordination Chemistry, Faculty of Chemistry, Maria Curie-Sklodowska University, Sq. M Curie-Sklodowska 2, 20-031 Lublin, Poland

J. Sarzynski
Institute of Physics, Maria Curie-Sklodowska University, Sq. M Curie-Sklodowska 1, 20-031 Lublin, Poland

form cationic octahedral complexes, which are known to have important biological properties [10].

Mixed-ligand coordination compounds of salicylaldehyde derivatives and α-diimines with transition metal ions, the structures of which are characterized by single crystal X-ray technique, are suitable to study different aspects of biological molecules and industrial application. Recently, our research group has reported that the Lewis acidity of $[Co^{II}(salo)_2]$ chelates renders them to be susceptible to nucleoplilic attack, and additional compounds can be obtained, such as $[Co(salo)_2(\alpha\text{-diimine})]$, where α-diimine = bipyridine(bipy), phenanthroline(phen) or neocuproine (neoc) [11–13].

As a continuation of this research, the structural and magnetic characterization and the thermal decomposition for two cobalt(II) compounds with neocuproine(neoc) and substituted salicylaldehydes(X-salo) (X = 3-OCH_3, or 5-CH_3) with the general formula [Co(X-salo)$_2$(neoc)] are described in this study, by using different techniques: Variable temperature magnetic susceptibilities, thermogravimetry (TG), differential thermal analysis (DTA) and TG unit coupled with MS spectroscopy by means of a heated transfer line in a proper temperature range up to 180 °C (TG-MS). For the calculation of the activation energy, the isoconversional Ozawa–Flynn–Wall (OFW) and the Friedman methods are used. The crystal structure of the compound [Co(3-OCH_3-salo)(neoc)] (**1**) was verified by the single-crystal X-ray diffraction analysis presented in this article, while for the compound [Co(5-CH_3-salo)$_2$(neoc)] (**2**), it has been published previously [12]. Recently, spectral and magnetic behaviour as well as crystal structure and thermal decomposition of transition metal or/and lanthanide complexes were investigated employing several techniques in conjunction with thermal analysis techniques [14–16].

Experimental

Instruments and methods

Microanalyses were carried out using a Perkin-Elmer 240 B CHN microanalyser and Perkin-Elmer 5100 PC Atomic Absorption Spectrophotometer for the metal content. Infrared spectra in the region of 4000–200 cm^{-1} were obtained in KBr discs with a Nicolet FT-IR 6700 spectrophotometer. Molar conductivities were measured in CH_3CN solutions, employing a WTW conductivity bridge and a calibrated dip type cell. Magnetic susceptibilities were investigated at 76–303 K with magnetic field strength of 9.9 kOe. The measurements were carried out using the Gouy method. Mass changes were obtained from Cahn RM-2 electrobalance. The calibrant employed was $Hg[Co(SCN)_4]$, for which the magnetic susceptibility was assumed to be 1.644×10^{-5} cm^{-3} g^{-1}. Correction for diamagnetism of the constituent atoms was calculated by the use of Pascal's constants [17].

The simultaneous TG/DTG-DTA curves were obtained on a SETARAM thermal analyser, model SETARAM SETSYS TG-DTA 16/18. Samples (6.0 ± 0.2 mg) were placed in alumina crucibles, and as reference was used an empty alumina crucible. The compounds were heated from ambient temperature to 1300 °C in a 50 ml/min flow of N_2, at several heating rates (5, 10, and 20 °C min^{-1}). For the TG-MS measurements TG was also carried out with a SETARAM thermal analyser, model SETSYS-1200. The samples of approximately 10 mg were heated in platinum crucibles, in an argon atmosphere at a flow rate of 80 ml min^{-1}, within the temperature range 30–1000 °C, at a heating rate of 10 °C min^{-1}. Mass spectra (MS) of the gaseous evolved moiety during the experiments were recorded since the TG apparatus was coupled with a quadrupole mass spectrometer (QMS) model Thermostar. The TG was linked to a heated gas cell of the MS by means of a heated transfer line, at temperature 180 °C. Data were processed using on line connected computer system with commercial software Quadstar. The structure identification of the residues is performed with X-ray diffraction analysis (XRD) using a 2-circle Rigaku Ultima$^+$ diffractometer (40 kV, 30 mA, CuKα radiation) with Bragg–Brentano geometry. Single-crystal diffraction data were collected at 130 K with a Kuma CCD single-crystal diffractometer equipped with an Oxford Cryostream device.

Materials and synthesis of the complexes [Co(X-salo)$_2$(neoc)] (**1–2**)

The ligands, 2-hydroxy-3-methoxy-benzaldehyde (3-OCH_3-salicylaldehyde), 2-hydroxy-5-methyl-benzaldehyde (5-CH_3-salicylaldehyde), 2,9-dimethyl,1,10–phenanthroline (neocuproine), and the metal salt $CoBr_2 \cdot 6H_2O$ were obtained as reagent grade from Aldrich and used as received. Solvents for preparation and physical measurements of 'extra pure' grade were obtained from Fluka without further purification.

The [Co(X-salo)$_2$(neoc)] complexes were prepared according to published procedures [12] by adding drop-wise a methanolic solution of 1 mmol substituted salicylaldehyde and 1 mmol CH_3ONa to a solution of $[Co(neoc)Br_2]$ (0.5 mmol) in H_2O at room temperature. The solution was stirred for 2 h and then turned darker, and an orange solid was formed. The solid was filtered, washed with water and dried under vacuo. All complexes were prepared under Argon conditions and well-degassed solutions have been used to avoid oxidation of the cobalt. Conductivities in CH_3CN solutions were found to have values between 1.8 and 6.7 μS/cm, denoting the neutral character of the compounds.

1. [Co(3-OCH_3-salo)$_2$(neoc)]: orange microcrystalline solid, yield 66.0%. Stoichiometry calculated for $C_{30}H_{26}CoN_2O_6$: C, 63.26; H, 4.57; Co, 10.37; N, 4.92. Found: C, 63.47; H, 4.47; Co, 10.12; N, 4.66%. IR spectrum (KBr): selected peaks in cm^{-1}: 2831 m ν(C–H) of the OCH_3, 1622 s ν(C=O), 1600 vs. ν(C=N), 848 m and 725 s (pyridyl C–H), 553 m (Co–O), 416 m (Co–N).

2. [Co(5-CH_3-salo)$_2$(neoc)]: orange solid, yield 63.0%. Stoichiometry calculated for $C_{30}H_{26}CoN_2O_4$: C, 67.04; H, 4.84; Co, 10.97; N, 5.21. Found: C, 66.67; H, 4.47; Co, 10.85; N, 5.47%. IR spectrum (KBr): selected peaks in cm^{-1}: 1625 s ν(C=O), 1596 vs. ν(C=N), 1462 m and 1397 m –ν(C–H) of the CH_3, 855 m and 728 s (pyridyl C–H), 550 m (Co–O), 410 m (Co–N).

X-ray crystal structure determination

Single crystals of (**1**) [Co(3-OCH_3-salo)$_2$(neoc)] were obtained from the reaction mixture after slow evaporation. Diffraction data were collected at 130 K with a KumaCCD single-crystal diffractometer equipped with an Oxford Cryostream device. Data collection and reduction were performed with CrysAlis CCD [18] and CrysAlis RED [18], respectively. The structure was solved by direct methods with the SHELXS–97 program [19] and refined by full–matrix least-squares method on F^2 with SHELXL–97 [20]. Hydrogen atoms were generated geometrically in idealized positions. Their displacement parameters were set equal to $1.5U_{eq}(C)$ for the methyl groups and $1.2U_{eq}(C)$ for the remaining H atoms. The crystal data and some details of the data collection and structure refinement are given in Table 1. CCDC 807486 contains the supplementary crystallographic data for this article.

Results and discussion

General considerations

The reaction of the [Co(neoc)Br_2] with two substituted salicylaldehydes (X-saloH) afforded in good yield very stably in air solid compounds. The characterization of their molecular structure was made by elemental analyses, conductivity and magnetic measurements, as well as by infrared spectroscopy [12]. The obtained cobalt(II) compounds are neutral and possess 1:2 metal-to-ligand composition, as it is indicated from elemental analyses and the absence of electrical conductivities in CH_3CN solutions. The complexes are formulated as [Co(X-salo)$_2$(neoc)], evidence also arisen from the interpretation of the IR data of the ligands (salicylaldehyde and neocuproine) and the complexes.

Table 1 Crystal data and structure refinement details for [Co(3-OCH_3-salo)$_2$(neoc)] (**1**)

Empirical formula	$C_{30}H_{26}CoN_2O_6$	
Formula weight	569.46	
Temperature/K	130 (2)	
Wavelenght/Å	0.71073	
Crystal system	Triclinic	
Space group	P − 1	
Unit cell dimensions	a = 10.6887(4) Å	α = 68.229(4)°
	b = 11.5576(5) Å	β = 69.333(3)°
	c = 11.6531(4) Å	γ = 87.367(3)°
Volume/Å^3	1244.87(10)	
Z	2	
Density calculated/g/cm^3	1.519	
F(000)	590	
Crystal size/mm^3	0.3 × 0.3 × 0.2	
θ range for data collection/°	2.01–27.74	
Limiting indices	$-13 \le h \ge 13$, $-14 \le k \ge 14$, $-14 \le l \ge 14$	
Reflection collected/unique	13670/5077	
Data/restraines/parameters	5077/0/356	
Completeness θ = 26.37°	99.6%	
Goodness-of-fit on F^2	1.042	
Final R indices [$I > 2\sigma(I)$]	$R_1 = 0.0259$; $wR_2 = 0.0664$	
R indices (all data)	$R_1 = 0.0348$; $wR_2 = 0.0706$	
$\Delta_{\rho max}$ and $\Delta_{\rho min}$/eÅ^{-3}	0.324 and −0.329	

Their magnetic moments at room temperature ($\mu_{eff} = \sim 4.12\ \mu_B$), corroborate with high-spin octahedral coordination of the Co(II) ion. The crystal structure of the studied compound [Co(3-OCH_3-salo)$_2$(neoc)] (**1**) was verified by single-crystal X-ray diffraction analysis presented here, while for the compound [Co(5-CH_3-salo)$_2$(neoc)] (**2**) it was recently confirmed [12] (Scheme 1a, b). In these compounds, the salicylaldehydes behave as bidentate monoanionic ligands, through the carbonyl and the phenolic oxygen atoms, while the neocuproine as bidentate neutral ligand, forming an octahedral geometry around cobalt. This knowledge provides a useful basis, for predicting the structure of the yet unknown analogous complexes.

Crystal structure of [Co(3-OCH_3-salo)$_2$(neoc)] (**1**)

The molecular structure of [Co(3-OCH_3-salo)$_2$(neoc)] (**1**), shown with the atom numbering scheme in Fig. 1, clearly indicates that the cobalt(II) atom is chelated by one neoc ligand and by two 3-OCH_3-salo ligands via the phenolic and carbonyl oxygen atoms, resulting in a distorted octahedral coordination geometry. Moreover, the geometrical isomer isolated from the reaction is that with the carbonyl groups placed *trans* to the neoc N atoms. The molecule of

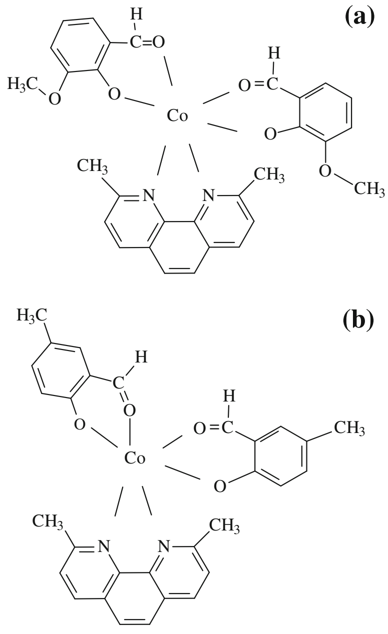

Scheme 1 **a** Molecular structure of [Co^{II}(3-OCH$_3$-salo)$_2$(neoc)] (**1**); **b** molecular structure of [Co^{II}(5-CH$_3$-salo)$_2$(neoc)] (**2**) [12]

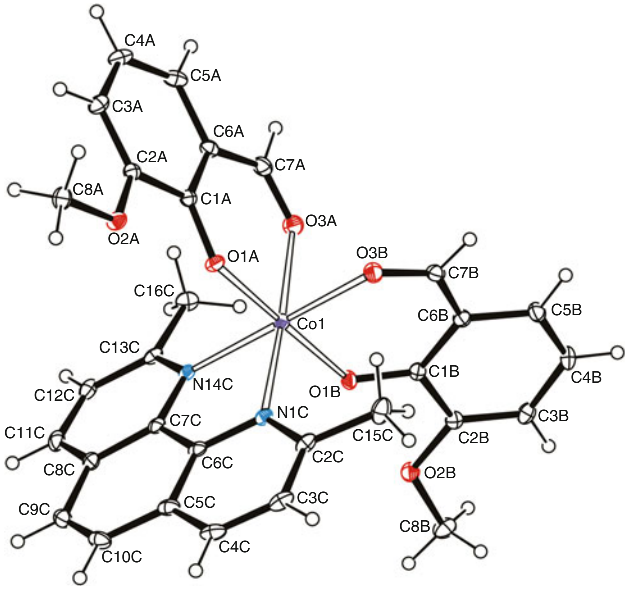

Fig. 1 Molecular structure of [Co(3-OCH$_3$-salo)$_2$(neoc)] (**1**) with the displacement ellipsoids shown at the 50% probability level

Table 2 Selected bond lengths/Å and angles/° for [Co(3-OCH$_3$-salo)$_2$(neoc)] (**1**)

Bond lengths			
Co(1)–O(1A)	2.0040(11)	N(14C)–C(7C)	1.360(2)
Co(1)–O(1B)	2.0278(11)	O(1A)–C(1A)	1.2855(18)
Co(1)–O(3A)	2.0844(11)	O(2A)–C(2A)	1.3687(19)
Co(1)–O(3B)	2.1407(11)	O(2A)–C(8A)	1.4236(19)
Co(1)–N(14C)	2.1723(13)	O(3A)–C(7A)	1.2366(19)
Co(1)–N(1C)	2.1728(13)	O(1B)–C(1B)	1.2874(18)
N(1C)–C(2C)	1.3373(19)	O(2B)–C(2B)	1.3670(19)
N(1C)–C(6C)	1.367(2)	O(2B)–C(8B)	1.4239(18)
N(14C)–C(13C)	1.342(2)		
Bond angles			
O(1A)–Co(1)–O(3A)	88.48(4)	O(3A)–Co(1)–N(14C)	102.33(5)
O(1B)–Co(1)–O(3A)	89.95(4)	O(3B)–Co(1)–N(14C)	175.56(4)
O(1A)–Co(1)–O(3B)	93.53(4)	O(1A)–Co(1)–N(1C)	91.68(4)
O(1B)–Co(1)–O(3B)	87.53(4)	O(1B)–Co(1)–N(1C)	89.89(5)
O(3A)–Co(1)–O(3B)	77.90(5)	O(3A)–Co(1)–N(1C)	179.78(5)
O(1A)–Co(1)–N(14C)	90.91(5)	O(3B)–Co(1)–N(1C)	101.94(5)
O(1B)–Co(1)–N(14C)	88.03(4)	N(14C)–Co(1)–N(1C)	77.81(5)
O(1A)–Co(1)–O(1B)	177.89(4)		

[Co(3-OCH$_3$-salo)$_2$(neoc)] (**1**), with the salo-type ligand chelating via the phenolic and carbonyl oxygen atoms, can exist in the form of three geometric isomers. Two isomers are C$_2$ symmetric with either phenolic or carbonyl O atoms positioned *trans* to the N atoms of the neoc ligand and the third isomer is asymmetric, with the phenolic O atom of one and the carbonyl O atom of the second 3-OCH$_3$-salo ligand in *trans* position to the neoc ligand. All complexes of the [Co(X-salo)$_2$(α-diimine)] type (α-diimine = bipy, phen, neoc) isolated so far are in the same geometrical form as the one observed in the crystal structure of (**1**) [Co(3-OCH$_3$-salo)$_2$(neoc)] [11, 12].

As should be expected, the Co–O bond lengths involving carbonyl O atoms are longer than the Co–O bond length involving phenolic O atoms (Table 2), and coordination geometry around Co(II) can be considered as axially compressed distorted octahedral with the phenolic O1A and O1B atoms occupying axial positions and N1C, N14C, O3A and O3B atoms situated in the equatorial plane. The Co(II) atom deviates from the equatorial plane by 0.043(2) Å. Owing to the steric effects of the two methyl substituents, the neoc ligand is inclined to the equatorial plane by 13.42(6)°, and therefore, the metal ion is displaced from the neoc best plane by 0.372(3) Å. In this propeller-type molecule, the dihedral angles between the best planes of the three planar chelating ligands are in the range of 69–82°. The packing of the molecules in the crystal is mostly determined by π-π stacking interactions between the α-diimine ligands and numerous C–H···O and C–H···π interactions.

Magnetic behaviour

The magnetic susceptibility of the analysed complexes was measured in the temperature range of 77–303 K. The complexes follow the Curie–Weiss law, since the values of their magnetic susceptibility decrease with increasing temperature. The paramagnetic dependences of magnetic susceptibility values of the compounds as a function of temperatures are presented in Figs. 2 and 3. The effective magnetic moment values were calculated from the equation: $\mu_{\mathrm{eff}} = 2.83(\chi_{\mathrm{M}}\mathrm{T})^{1/2}$ where: μ_{eff} is the effective magnetic moment, χ_{M} is the magnetic susceptibility per molecule and T is the absolute temperature. The magnetic moment values experimentally determined for [Co(3-OCH_3-salo)$_2$(neoc)] (**1**) in the range of 77–303 K change from 3.88 μ_β (76 K) to 4.14 μ_β (303 K) while its value for [Co(5-CH_3-salo)$_2$(neoc)] (**2**) at room temperature is equal to 4.08 μ_β. These μ_{eff} values are higher than that for the spin-only value calculated for the free Co(II) ion from the equation $\mu_{\mathrm{eff}} = [4S(S+1)]^{1/2}$ in the absence of the magnetic interactions for present spin-system [21, 22]. The magnetic moment theoretically calculated for Co(II) ion at room temperature is equal to 3.88 μ_β [23, 24].

The difference between the measured and calculated values of magnetic moments may result from a spin-orbital coupling [24], or from the ferromagnetic alignment of the spins in the complex molecular centres and difference of geometry of paramagnetic centre surroundings [25]. The experimental magnetic data confirm the results obtained from the X-ray single crystal structure determination. The magnetic moment values indicate that the analysed compounds of Co(II) ions are high-spin complexes with weak ligand fields and octahedral coordination of central ion according to those of analogous types and with coordination number equal to six [26, 27]. In the case of [Co (3-OCH_3-salo)$_2$(neoc)] (**1**) in the octahedral coordination of Co(II) ion sphere, there are four oxygen atoms of two salicylaldehyde molecules and two nitrogen atoms coming from one neocuproine molecule (Fig. 1).

The difference in the magnetic moment values determined for those two analysed complexes may probably result from the slight differentiated molecular and crystal structure of both forms connected with the changes in geometry of the octahedral Co(II) ion coordination spheres [22, 25].

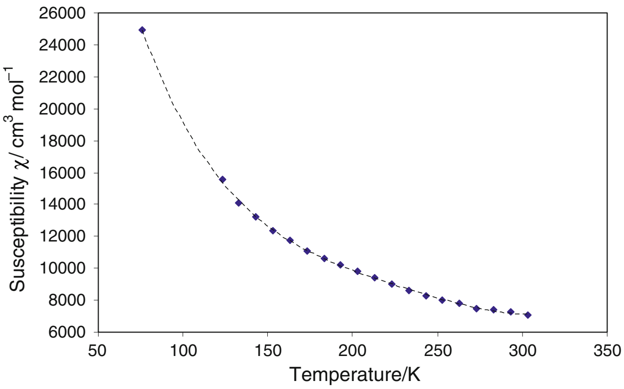

Fig. 2 Dependence between magnetic susceptibility values vs. temperature for [Co(3-OCH_3-salo)$_2$(neoc)] (**1**)

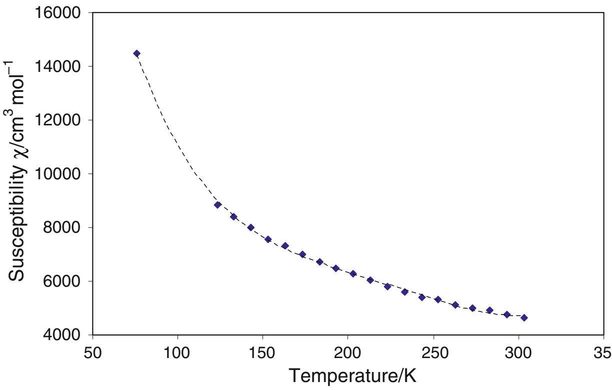

Fig. 3 Dependence between magnetic susceptibility values vs. temperature for [Co(5-CH_3-salo)$_2$(neoc)] (**2**)

Thermal decomposition

TG/DTG-DTA in nitrogen

Thermoanalytical curves (TG/DTG-DTA) for the compounds [Co(3-OCH_3-salo)$_2$(neoc)] (**1**) and [Co(5-CH_3-salo)$_2$(neoc)] (**2**) in nitrogen atmosphere at heating rate 10 °C min^{-1} are given in Figs. 4 and 5, respectively.

Their decomposition profile is similar, while the shape of the mass loss is very complicated. It presents four different areas of mass loss and each area starts before the ending of the previous one. For this reason, it is very difficult to correspond to different areas of mass loss in a specific way of decomposition of the compound. Using mass loss and derivative mass loss plots (TG/DTG), we can conclude that: under nitrogen, in the first stage (120–250 °C), the compound [Co(3-OCH_3-salo)$_2$(neoc)] (**1**) (Fig. 4) shows sudden mass loss (DTG peak at 192 °C) of 5.8%, which coincides with the release of one formaldehyde molecule (H_2CO) with a theoretical mass loss of 5.27%. The DTA curve shows one sharp endothermic peak at 188 °C, which is attributed to melting followed by decomposition. The melting points of the studied compounds were also determined by automated melting point capillary tube system in static air confirming the melting points found on the DTA curves.

Upon increasing the temperature, the unstable intermediates undergo further decomposition with gradual mass loss during the second and third stages as follows: second stage (250–476 °C, DTG peaks at 319 and 374 °C, DTA peak exothermic at 361 °C, mass loss of 10.3%) and third stage (476–687 °C, DTG peak at 527 °C, mass loss of 17.5%). The fourth stage is more rapid (687–800 °C, DTG peak at 742 and DTA, sharp exothermic at 740 °C with mass loss of 8.5%). The mass loss of the second, third and

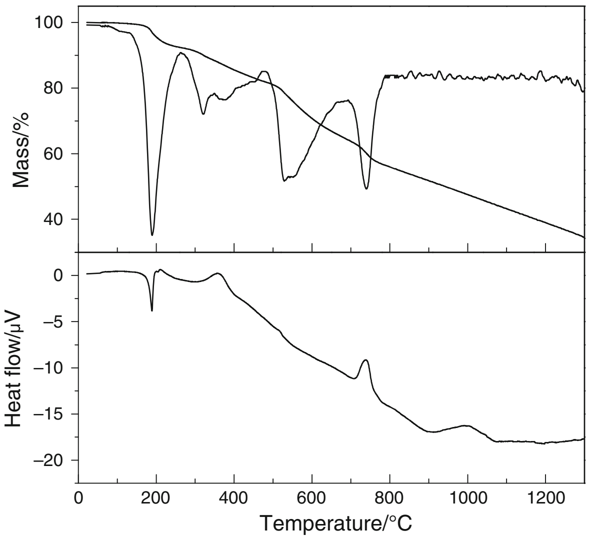

Fig. 4 Thermoanalytical curves (TG/DTG-DTA) of [Co(3-OCH_3-salo)$_2$(neoc)] in nitrogen. Heating rate 10 °C min $^{-1}$ (**1**)

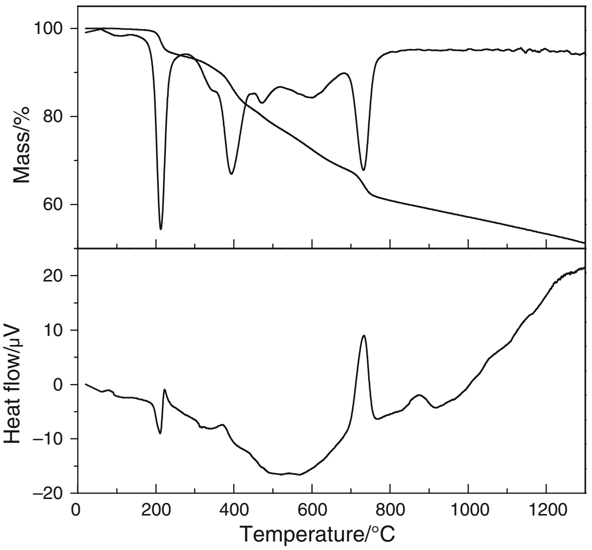

Fig. 5 Thermoanalytical curves (TG/DTG-DTA) of [Co(5-CH_3-salo)$_2$(neoc)] in nitrogen. Heating rate 10 °C min $^{-1}$ (**2**)

fourth stages are attributed to the elimination of the remaining organic parts of the ligands. Efforts to isolate the intermediates were not successful because of their continuous decomposition, as it was evidenced from the TG curves, while the mass losses at these stages cannot be attributed to certain species. The amount of the solid material estimated from the TG curve, was found 30.0% and denotes that the decomposition of this compound at 1300 °C was not completed, since the calculated value for the expected metallic cobalt is 10.33% and for CoO 13.13%.

For compound (**2**) [Co(5-CH_3-salo)$_2$(neoc)] (Fig. 5), the mass loss of 6.0% of the first stage (153–270 °C, DTG peak at 213 °C) can also be attributed to the elimination of a formaldehyde molecule (calculated 5.58%). The DTA curve shows one sharp endothermic peak at 210 °C and an exothermic one at 220 °C, because of the melting and decomposition of the compound.

Upon increasing the temperature, the unstable intermediates undergo further decomposition with gradual mass loss during the second and third stages as follows: second stage (270–450 °C, DTG peak at 394 °C, DTA peak exothermic at 370 °C, mass loss of 11.8%) and third stage (450–684 °C, DTG peaks at 480 and 598 °C, mass loss of 13.6%). The fourth stage is more rapid (684–811 °C, DTG peak at 730 and DTA, sharp intense exothermic at 734 °C with mass loss of 7.4%). The amount of the solid material at 1300 °C estimated from the TG curve, was found 49% and is much higher than the calculated for the metallic cobalt 10.94% or for the cobalt oxide CoO 13.91%. This fact suggests that the thermal decomposition residue consists from a carbonaceous mixture, resulting from the uncompleted pyrolysis of the compound.

The complex nature of thermal decomposition for analogous cobalt complexes has also recently been referred [28, 29]. In order to verify the solid residues, as they are deduced and estimated from the TG and DTG curves of the studied cobalt compounds, powder XRD studies were used. It was found that the solid material, at 1300 °C consists from cubic metallic cobalt (Supplementary material, Fig. 1s).

An attempt to clarify the thermal decomposition released gases for both cobalt compounds, the TG-MS technique in argon atmosphere was employed. The detected mass for the first stage with m/z: 30 could be assigned to formaldehyde (H_2CO), while for the second, the masses m/z: 16, 17 and 18 are assigned to methane (CH_4), ammonia (NH_3) and water vapour (H_2O), respectively. For the third and fourth stages, however, there are not obvious peaks and only a broad band with low ion current and m/z: 44 could be assigned to carbon dioxide (CO_2). The existence of the carbon dioxide could explain the exothermic nature of the decomposition, possibly due to the oxidation of the released carbon monoxide.

Kinetic analyses

In order to determine the kinetic mechanisms of the decomposition of the studied materials, different heating rates were used. The mass loss for heating rates 5, 10, and 20 °C min^{-1} are shown in Figs. 6 and 7 for the compounds **1** and **2**, respectively. The onset shifts to higher temperatures with increasing β because of the shorter time required for the sample to reach a given temperature at faster heating rates. In addition, the total mass loss is higher in the case of small heating rates, such as $\beta = 5$ °C min^{-1},

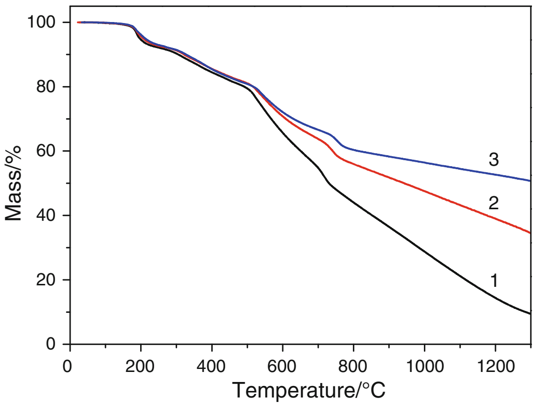

Fig. 6 Mass loss curves of [Co(3-OCH$_3$-salo)$_2$(neoc)] (**1**) in nitrogen, with different heating rates (*1* $\beta = 5$ °C min^{-1}, *2* $\beta = 10$ °C min^{-1}, *3* $\beta = 20$ °C min^{-1})

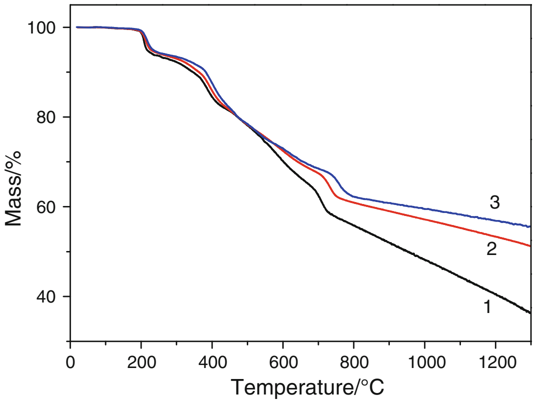

Fig. 7 Mass loss curves of [Co(5-CH$_3$-salo)$_2$(neoc)] (**2**) in nitrogen, with different heating rates (*1* $\beta = 5$ °C min^{-1}, *2* $\beta = 10$ °C min^{-1}, *3* $\beta = 20$ °C min^{-1})

resulting in the completion of the decomposition and the obtainment of the pure metal cobalt as final residue at 1300 °C, especially in case of compound (**1**).

As it can be seen in Figs. 6 and 7 above 500 °C, for both materials, the quantity of mass loss depends on the heating rate. For this reason, the quantity of the residue varies very much, possibly due to the big amount of organic carbon derived from the fragmented ligand, which can be completely pyrolized only in a small heating rate. So, the dependence of the activation energy has been calculated only for the temperature area 20–500 °C.

For the determination of the activation energy by using multiple heating rates, the isoconversional methods are used. Since every isoconversional method has different error, the use of more than one method can give a range of values for the activation energy at every particular value of α.

The OFW [30, 31] method involves the measurement of the temperature T, corresponding to a fixed value of the degree of conversion α, from the experiments at different heating rates β. The OFW method is based on the following equation:

$$\ln \beta = -1.0516 \frac{E}{RT} + \text{const}$$

where, A is the pre-exponential factor, E the activation energy, β the heating rate and R the gas constant. The plot of lnβ vs. 1/T gives the slope -1.0516 E/R by which the activation energy has been evaluated. If the determined activation energy is the same for the various values of α, the existence of a single-step reaction can be concluded with certainty. On the contrary, a change of E with increasing degree of conversion is an indication of a complex reaction mechanism that invalidates the separation of variables involved in the OFW analysis [32]. These complications are significant, especially in the case that the total reaction involves competitive mechanisms.

The second method that was employed is the differential isoconversional method suggested by Friedman [33], and it is based on the following equation:

$$\ln\left(\beta \frac{\mathrm{d}\alpha}{\mathrm{d}T}\right) = \ln A + \ln f(\alpha) - \frac{E}{RT}$$

where, α is the degree of conversion and $f(\alpha)$ the conversion function (reaction model). For a constant α, the plot of $\ln(\beta(\mathrm{d}\alpha)/(\mathrm{d}T))\mathrm{vs.}(1/T)$ obtained from curves recorded at several heating rates, should be a straight line, the slope of which gives us the value of E. It is obvious from the above equation that if the function $f(\alpha)$ is constant for a particular value of α, then the sum ln$f(\alpha)$ + lnA/β is also constant.

In Figs. 8 and 9, the dependence of the activation energy on the different conversion values as calculated by the OFW and Friedman methods is presented.

As it can be seen for both materials, the dependence of the activation energy is very complicated. It presents more than two different areas of stable values or monotonous

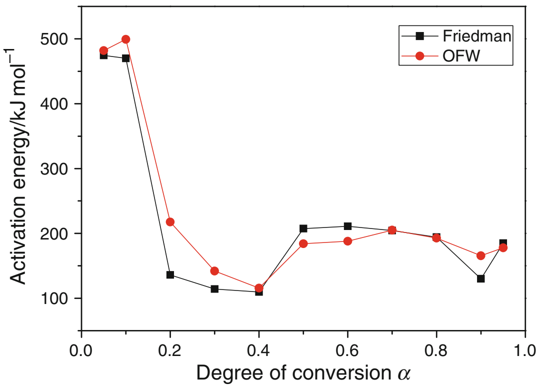

Fig. 8 Activation energy E, as calculated with OFW and Friedman methods, vs. degree of conversion α for compound (1) [Co(3-OCH$_3$-salo)$_2$(neoc)]

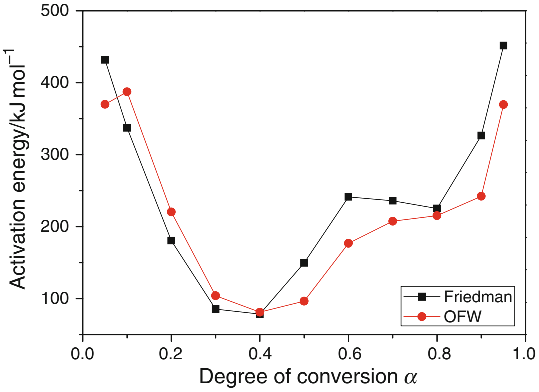

Fig. 9 Activation energy *E*, as calculated with OFW and Friedman methods, vs. degree of conversion α for compound (2) [Co(5-CH_3-salo)$_2$(neoc)]

increase or decrease. This is a strong indication that for the kinetic description of the decomposition of these materials must be used more than two different kinetic mechanisms. The calculation of the activation energy using more than one isoconversional methods can give an area of values for every particular value of α, where the true values of *E* can be found. The differences in the values of *E* calculated by the OFW and Friedman methods can be explained by a systematic error because of improper integration. The method of Friedman employs instantaneous rate values being measured; therefore, it appears to be very sensitive to experimental noise. With OFW method, the equation used is derived assuming constant activation energy and by introducing systematic error in the estimation of *E* in the case that *E* varies with α, an error that can be estimated by comparison with the Friedman results [34].

Conclusions

Two neutral complexes, under the formula [Co(X-salo)$_2$ (neoc)], were prepared and characterized. Octahedral arrangement of the ligands around cobalt(II) metal ion was verified by the single-crystal X-ray diffraction analysis for both of them (this article and [12]).

The variable temperature magnetic susceptibility measurements revealed the paramagnetic nature of the title cobalt(II) complexes. The compounds follow the Curie–Weiss law, since the values of the magnetic susceptibility decrease with the increase of the temperature.

Their decomposition profile is similar, while the shape of the mass loss is very complicated. It presents four different areas of mass loss, and each area starts before the ending of the previous one. The decomposition of the complexes is not completed in nitrogen atmosphere up to 1300 °C, and the solid material found at this temperature is a mixture of carbonaceous metal cobalt, verified by PXRD.

The *E* was calculated with two different methods, the isoconversional methods of OFW, and Friedman. The dependence of the activation energy is very complicated. It presents more than two different areas of stable values or monotonous increase or decrease. This is a strong indication supporting that for the kinetic description of the decomposition of these materials, more than two different kinetic mechanisms must be used.

Supplementary data

Detailed crystal data and structure refinement for complex [Co(3-OCH_3-salo)$_2$(neoc)] have been deposited with the Cambridge Crystallographic Data Centre under No CCDC 807486. Copies of this information may be obtained free of charge from the Director, CCDC, 12 Union Road, Cambridge, CB2 IEZ, UK (fax: +44-1223-336033; e-mail: deposit@ccdc.cam.ac.uk or http://www.ccdc.cam.ac.uk). XRD pattern of the thermal decomposition residue at 1400 °C in N_2, for compounds **1** and/or **2** is also given as supplementary material in Fig. 1s.

References

1. Prasad RN, Agrawal A. Synthesis and spectroscopic studies of mixed ligand complexes of cobalt(II) with salicylaldehyde, hydroxyarylketones and beta-diketones. J Indian Chem Soc. 2006;83(1):75–7.
2. Hussain ST, Ahmad H, Atta MA, Afzal M, Saleem M. High performance liquid chromatography (HPLC), atomic absorption spectroscopy (AAS) and infrared spectroscopy determination and solvent extraction of uranium, using bis(salicylaldehyde) propylene diamine as complexing agent. J Trace Microprobe Tech. 1998;16(2):139–49.
3. Sajith P, Ummer MT, Mandal N, Mandot SK, Agrawal SL, Bandyopadhyay S, Mukhopadhyay R, D'Cruz B, Deuri AS, Kuriakose P. Synthesis of cobalt complexes and their evaluation as an adhesion promoter in a rubber-steel wire system. J Adhesion Sci Technol. 2005;19(16):1475–91.
4. Sun Y-X, Gao G-Z. Bis(4-bromo-2-formylphenolato-κ^2 O,O′) copper(II). Acta Cryst. 2005;E61(2):m354–5.
5. Chen Q. Bis(4-bromo-2-formylphenolato-κ^2 O,O′)zinc(II). Acta Cryst. 2006;E62(1):m56–7.
6. Yang Y-M, Lu P-C, Zhu T-T, Liu C-H. Bis(2-formylphenolato-κ^2 O,O′)iron(II). Acta Cryst. 2007;E63(6):m1613.
7. Pessoa JC, Cavaco I, Correira I, Tomaz I, Duarte T, Matias PM. Oxovanadium(IV) complexes with aromatic aldehydes. J Inorg Biochem. 2000;80(1):35–9.
8. Lalia-Kantouri M, Papadopoulos CD, Hatzidimitriou AG, Skoulika S. Hetero-heptanuclear (Fe–Na) complexes of salicylaldehydes: crystal and molecular structure of [Fe_2(3-OCH_3-salo)8/Na_5]·3OH·8H_2O. Struct Chem. 2009;20(2):177–84.
9. Lalia-Kantouri M, Dimitriadis T, Papadopoulos CD, Gdaniec M, Czapik A, Hatzidimitriou AG. Synthesis and structural characterization of iron(III) complexes with 2-hydroxyphenones. Z Anorg Allg Chem. 2009;635(13):2185–90.

10. Bedell SA, Martell AE. Oxidation of 2,6-di-tert-butylphenol by molecular oxygen. Catalysis by tetrakis(bipyridyl)(μ-peroxo)(μ-hydroxo)dicobalt(III). Inorg Chem. 1983;22(2):364–7.
11. Papadopoulos CD, Hatzidimitriou AG, Voutsas GP, Lalia-Kantouri M. Synthesis and characterization of new addition compounds of bis(substituted-salicylaldehydo) cobalt(II) with 2,2′-bipyridine (bipy). Crystal and molecular structures of [Co^{II}(3-methoxy-salicylaldehyde)$_2$(bipy)]·CH_3OH (1) and [Co^{II}(bipy)$_3$]Br_2·0.5(5-chloro-salicylaldehydeH). 1.5CH_3OH (5). Polyhedron. 2007;26(5):1077–86.
12. Papadopoulos CD, Lalia-Kantouri M, Jaud J, Hatzidimitriou AG. Substitution effect on new Co(II) addition compounds with salicylaldehydes and the nitrogenous bases phen or neoc: crystal and molecular structures of [Co^{II}(5-NO_2-salicylaldehyde)$_2$(phen)], [Co^{II}(5-CH_3-salicylaldehyde)$_2$(neoc)] and [Co^{II}(5-Cl-salicylaldehyde)$_2$(neoc)]. Inorg Chim Acta. 2007;360(11):3581–9.
13. Papadopoulos CD, Hatzidimitriou AG, Quirós M, Sigalas MP, Lalia-Kantouri M. Synthesis, characterization, thermal and theoretical studies of cobalt(II) addition compounds with 2-hydroxyphenones and α-diimines. Crystal and molecular structures of [Co(2-hydroxy- benzophenone)$_2$(bipy)]·2-hydroxy-benzophenoneH (3) and [Co(2-hydroxy- benzophenone)$_2$(phen)] (8). Polyhedron, 2011; 30(3):486–96. doi:10.1016/j.poly.2010.11.010.
14. Curtis SA, Kurdziel K, Materazzi S, Vecchio S. Crystal structure and thermoanalytical study of a manganese(II) complex with 1-allylimidazole. J Therm Anal Calorim. 2008;92(1):109–14.
15. Dziewulska-Kulaczkowska A, Mazur L, Ferenc W. Thermal, spectroscopic and structural studies of zinc(II) complex with Nicotinamide. J Therm Anal Calorim. 2009;96(1):255–60.
16. Ye HM, Ren N, Li H, Zhang JJ, Sum SJ, Tian L. Synthesis, crystal structure and thermal decomposition kinetics of complex [Nd(BA)$_3$bipy]$_2$. J Therm Anal Calorim. 2010;101(1):205–11.
17. Figgis BN, Nyholm RS. A convenient solid for calibration of Gouy magnetic susceptibility apparatus. J Chem Soc. 1958; 4190:1.
18. Oxford Diffraction program name(s), CrysAlis CCD and CrysAlis RED Ver.1.171.31. Abingdon, Oxfordshire, England: Oxford Diffraction Ltd.; 2006.
19. Sheldrick GM. SHELXS-97, program for solution of crystal structures, and SHELXL-97 program for crystal structures refinement. Göttingen: University of Göttingen; 1997.
20. Sheldrick GM. A short history of SHELX. Acta Cryst. 2008;A64:112–22.
21. O'Coonor JCh. Progress in inorganic chemistry. New York: Wiley; 1982. p. 204–83.
22. Martin RL. New pathways in inorganic chemistry. Cambridge: Cambridge University Press; 1968. p. 149–231.
23. Figgis NB, Lewis J. Progress in inorganic chemistry. New York: Interscience; 1964. p. 37.
24. Burger K. Coordination chemistry: experimental methods. Budapest: Akademiai Kiado; 1973.
25. Earnshaw A. Introduction to magnetochemistry. London: Academic Press; 1968.
26. Cotton FA, Wilkinson G. Advanced inorganic chemistry. New York: Wiley; 1988. p. 730.
27. Patel KN, Patel NH, Patel KM, Patel MN. Synthesis and characterization of cobalt(II), nickel(II), copper(II) and zinc(II) mixed-ligand complexes. Synth React Inorg Metal Org Chem. 2000;30(5):921–30.
28. Ferenc W, Cristvao B, Sarzynski J. Thermal and magnetic behavior of 5-chloro-2-nitrobenzoates of Co(II), Ni(II) and Cu(II). J Therm Anal. 2010;101(2):761–7.
29. Dziewulska-Kulaczkowska A. Manganese(II), cobalt(II), nickel(II), copper(II) and zinc(II) complexes with 4-oxo-4H-1-benzopyran-3-carboxaldehyde: thermal, spectroscopic and magnetic characterization. J Therm Anal. 2010;101(3):1019–26.
30. Flynn JH, Wall LA. A quick direct method for the determination of activation energy from thermogravimetric data. J Polym Sci B Polymer Lett. 1966;4(5):323–8.
31. Ozawa T. A new method of analyzing thermogravimetric data. Bull Chem Soc Jpn. 1965;38(x):1881–6.
32. Ozawa T. Kinetic analysis of derivative curves in thermal analysis. J Therm Anal. 1970;2(3):301–24.
33. Friedman HL. Kinetics of thermal degradation of char-forming plastics from thermogravimetry. Application to a phenolic plastic. J Polym Sci C. 1964;6(x):183–95.
34. Vyazovkin S. Modification of the integral isoconversional method to account for variation in the activation energy. J Comput Chem. 2001;22(2):178–83.